EasyChair Preprint

№ 7315

A Speculative Approach to Efficiently Harvesting Sustainable Energy

Rubaiat Hossain, Faiyaz Fahim and Sabid Hasan

January 10, 2022

A Speculative Approach to Efficiently Harvesting Sustainable Energy

Rubaiat Hossain[1], Faiyaz Fahim[1*], Sabid Hasan[1]

[1]Department of Electrical & Electronic Engineering, Bangladesh Army University of Engineering & Technology, Qadirabad, Natore-6431, Bangladesh

Abstract: Energy demand will never decline in the same way as it did when the industrial revolution began and continued to flourish on energy use. The widespread use of fossil fuels leads to major environmental problems such as global warming, air and water pollution, and also has a detrimental influence on human health. Finding a safe and sustainable alternative energy source has become a sine qua non for human beings. We considered many methods for developing an energy source that could be used to generate electricity without relying on fossil fuels in both on- and off-grid circumstances. We intended to build a system that would merge two current technologies and would offer strategies for boosting their power generation efficiency. To begin, we examined tandem perovskite-silicon photovoltaic (PV) cells. Due to efficiency losses caused by heat and the module's inability to monitor the sun's direction for optimum irradiation capture, the necessity for a cooling unit and solar tracker became obvious, as did its functioning at night. An ancient technique known as Radiative Sky Cooling (RSC) was recently reintroduced to our understanding as a result of fast advances in nano-optics, nano-fabrication, and metamaterials. It can cool a system by boosting radiative heat transfer with cold space in the 8 to 13 m atmospheric window. Due to the fact that this system can now operate in direct sunlight, we investigated the subject, watched its operation, and examined if a single arrangement consisting of RSC and PV cells was conceivable. Using a thermoelectric generator as an RSC enables nighttime power generation, but at a poor efficiency, which we investigated and hypothesized several ways to enhance.

Keywords: *Radiative Sky Cooling, Solar Tracker, Photovoltaic, Thermoelectric Effect, Renewable Energy Source.*

Introduction: Consumption of fossil fuels, e.g., CO_2, CH_4, and N_2O (three most potent gases that prompt 98% of the global GHG emissions considered by The Kyoto Protocol*) for energy production, agriculture, transportation, and industrial applications is accelerating climate change as we speak. These economic activities, i.e., energy production, agriculture and other land use, transportation, and industrial application, account for consecutively 25, 24, 14, 21 percent of the global GHG emissions [1]. Since the effects of climate change are not immediately evident, there is a lack of awareness about it in a vast portion of the global demographic. OECD believes that it is a global systemic risk to society [2]. Severe effects

such as continual rise in temperature, frost-free season, lengthening of the growing season, changes in precipitation patterns, an increase of droughts and heatwaves, strengthening of hurricanes and other natural extremities, rising of sea-level and melting of ice in the arctic region could very well hamper not only the global economy but also the overall development of human civilization [3, 4, 5]. The possible damage to our economy could very well equate to a permanent loss in average per capita world consumption of more than 14% [6].

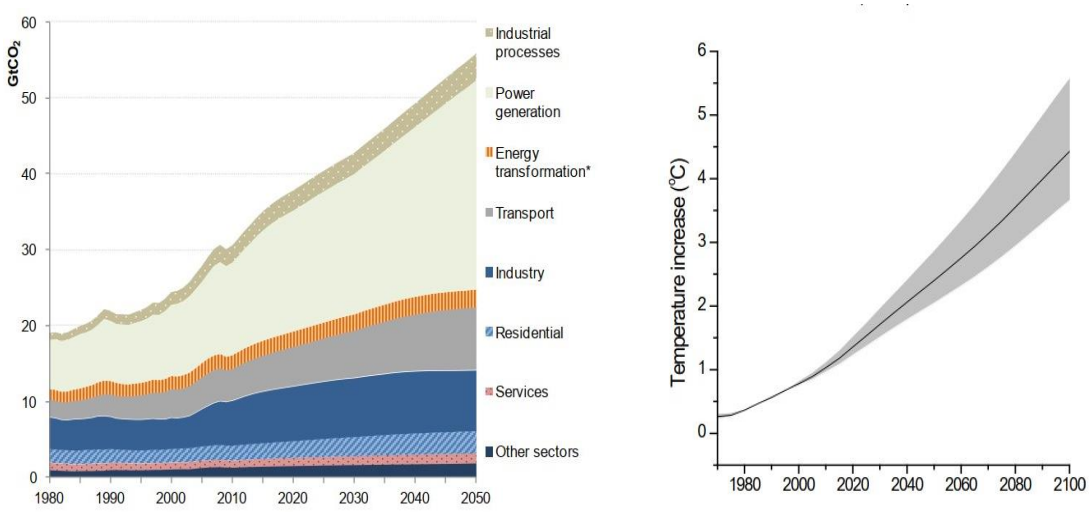

Note: Adapted from [7]. The category "energy transformation" includes emissions from oil refineries, coal and gas liquefaction.
GtCO2e = Gigatonnes of CO_2 equivalent.
Source: OECD Environmental Outlook Baseline; output from IMAGE.

Fig.1: Global Emissions by source (1980-2050) and Projected Temperature Increase (1980-2100).

The need for renewable energy sources becomes apparent from these statistics. Photovoltaics, thermal photovoltaics, and other solar thermal technologies rose over the last century, which harvests (Energy harvesting represents the energy derived from ambient sources that are extracted and directly converted into electrical energy [8].) the sun's energy are regarded as sustainable alternatives to fossil fuel. However, these techniques are depended on daylight; there were no feasible methods of harvesting energy during the night when energy demand actually peaks. But recently, a heat engine has been proposed that exploits the ambient air surrounding the earth's surface and the cold of outer space. The first successful implementation was demonstrated in a device that paired the cold side of a TEG (Thermoelectric Generator; a device consisting of one or multiple thermocouples, generates energy based on a temperature gradient) to a sky-facing blackbody surface that radiates heat

to the cold space and has its hot side heated by ambient air, generating 25 mW/m^2 power at night [9]. The basic operating diagram of a TEG is shown in figure 2. By optimization of the radiative cooler, environmental convection and figure-of-merit ZT (which used to characterize a thermoelectric material performance, as well as the efficiencies of various TEGs working at the same temperatures and dependent upon thermal conductivity *k* and electrical conductivity $\sigma = {}^{1}/_{\rho}$ [10]) of this device, a model was shown with a power generation capability of 2.2 W/m^{2,} which is approximately 88 times of the device shown in [9]. Our proposed theoretical system uses this optimized nighttime TEG device and amalgamates it into a structure that could also make use of solar energy during the day. Acrylic Fresnel lenses, a selective absorber, a dual-axis tracking system are necessary components for restructuring the TEG during the presence of daylight into a STEG. L. L. Baranowski et al. mentioned and analyzed a STEG model with an incident flux of 100 kW/m^2 (100 suns) and a hot side temperature of 1000 °C. The use of Perovskite has been on the increment since 2012, which has light photon-to-electron conversion efficiencies over 10% [30]. Since then, the sunlight-to-electrical-power conversion efficiency of Perovskite solar cells has skyrocketed. With the laboratory record standing at 25.2%, Perovskite-based tandem cells are being used nowadays for their price is predicted to go down in the near future, making them highly efficient alternatives to conventional silicon solar cells. Perovskite-based solar cells incorporated with an effective cooling system will be working along the TEG for our proposed system. We observe the power density, efficiency, and other independent module parameters and provide a hypothetical schematic of the modular arrangement in our paper.

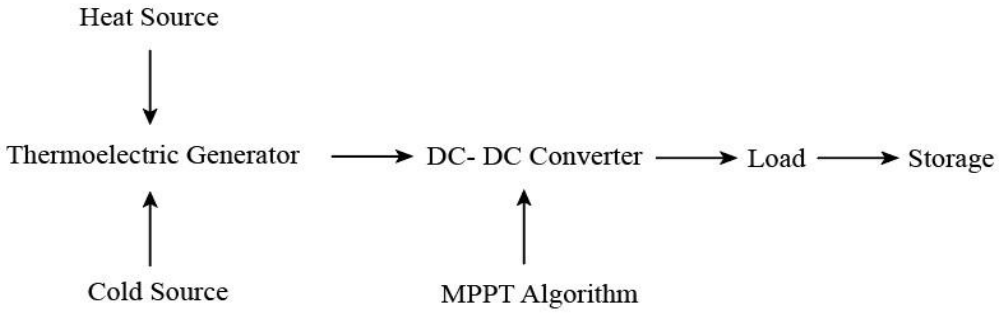

Fig.2: Diagram of TEG Operation.

Materials and Methods: In this section, we elucidate the analysis of energy production at night of the TEG, mathematical evidence, and effects of different parameters pertaining to the design of the TEG and STEG. Afterward, we clarify the PV module concepts with a cooling system and solar tracker, which are used in our conceptual modular arrangement.

A TEG converts heat energy into electrical energy according to the Seebeck effect, operates silently, under high maximum temperatures (up to 250 °C); uses reliable solid-state devices; does not require any maintenance, and is highly eco-friendly [8]. General TEGs have a conversion efficiency of 5-15% [12]. Nevertheless, when we discuss thermal energy harvesting, TEGs have an efficiency of about 5-6%. Energy conversion of TEGs is dependent on k, σ, and α, where α is the Seebeck coefficient and can be written as $\alpha = \frac{E}{\nabla T} = -\frac{V}{\nabla T}$. At night, for our TEG module, we closely follow the specifications and parameters mentioned in [13]. A multi-layered emitter shown in figure 3(a) is used to improve power generation performance. The emitter is optimally engineered in the spectro-angular domain so that it can give strong emission at frequencies ranging from 8-13μm spectrum where atmospheric absorption and ozone layer reflection are relatively small, the angular selectivity prevents emission at significant incident angular ranges for reasons like the opaque sky and downwards sky radiation. The optimal emissivity calculated by L Fan et al. was not realistically achievable, but the multi-layered emitter has a performance close to it and much higher than the one mentioned in [9], the air is chosen as the superstrate, and the multi-layered structure is placed on top of a 300nm (0.3 microns) Al layer. The emissivity, $\varepsilon \approx 1$; thermocouple effective area A_{TE} = 30x30 mm^2 (Marlow TG12-4-01LS) mentioned in [9]; the cold side surface area is, A_c= ATE/0.0156 = 0.058 mm^2, where 0.0156 is the optimal TE/Cooler Area ratio as predicted by L Fan et al.; the maximum generated power, P_{max} = 1.2144 W/m^2 which is 48 times higher than the outcome of [9], maximum power P_{max} can be calculated using: $\frac{n\,(\alpha.\Delta T)^2}{4RA_c}$ (Wm^{-2})where $R = n.[\rho_P.L_P(S_P)^{-1} + \rho_N.L_N(S_N)^{-1}$ is the internal resistance of a single thermocouple and $\rho = R.\,S/L$ is the specific resistance, S is the cross-sectional area of each leg, *k* is the thermal conductance; current $I = \frac{\alpha.\Delta T}{n.R+R_L}$ Where R_L is the external resistance; $h_c = 10^{-3}$ W/m^2k, $h_h = 10^2$ W/m^2k are the air convective transfer coefficients for the hot side and cold side (the value of h_h by using a heat-sink attached to the hot side in order to increase the effective area for convection by a factor of 10). The hot side of the TEG is assumed to have very low emissivity and is separated from other thermal reservoirs [13].

In the presence of daylight, the TEG is transformed into a concentrated STEG by replacement of the multi-layered emitter with the use of a small robotic lifter consisting of multiple linkages connected to a servo motor. The incident flux after passing through the concentrator is a function of the flux time's concentrator ratio [11]. For the concentrator, an Acrylic Fresnel lens was chosen, a selective absorber with an area of 1.6 cm^2 would have to be used for maximum efficiency [28, 29]. When operating a STEG, the upper side is chosen to be the hot side with a three-layered structure consisting of Bi_2Te_3, Skutterdite, and $Yb_{14}MnSb_{11}$/ La_3Te_4, which together gives a ZT = 1.03 showed in figure 3(b).

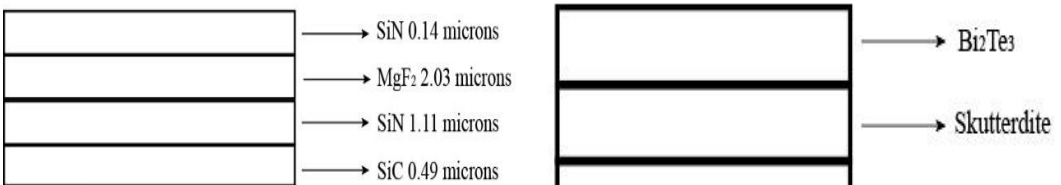

(a) (b)

Fig.3: (a) Multilayer Emitter for TEG, (b) Upper Layer for TEG at Day.

For the PV module, we decided to use monolithically connected integrated solar cells consisting of seven layers as suggested in [14]. Methylammonium bromide iodide lead ($CH_3NH_3PbI_{3(1-x)}Br_{3x}$ ($0 \leq x \leq 1$)) perovskite a type of hybrid organic-inorganic Perovskite (HOP) for the material used in top sub-cell, silicon as the bottom sub-cell material while a silicon tunnel junction (Si n++/ Si p++) (TJ) that connects the two layers was used. The optimal parameters for the HOP layer found from the simulations of A. Rolland et al., was selected which are thickness = 400 nm, x = 20% =0.02 in $CH_3NH_3PbI_{3(1-x)}Br_{3x}$ ($0 \leq x \leq 1$), bandgap energy, E_g = 1.7 eV, relative permittivity, ε_r = 6.5, electron and hole mobility, μ_n, μ_p = 2, electron and hole lifetime, τ_n, τ_p = 10^{-6}. The numerical data obtained from the simulations prove the potential of methylammonium bromide iodide lead as an absorbing material because of its relatively high efficiency and open-circuit voltage, low cost, and capability of being able to be fine-tuned in comparison to expensive GaAs and Ge substrates used in multi-junction solar cells (MJSC) mentioned in [15,16,17]. The specifications provided in [14] have a good current matching with the bottom cell, which depends on the absorber layer E_g and thickness. The tunnel junction has a doping level of 10^{20} $cm^{-3,}$ functioning as an ideal interconnection with low resistance due to silicon's high doping capacity. The effects of photons in HOP are similar to that in silicon, for which the existing drift-diffusion model could be implemented, while the final efficiency of the tandem cell was calculated as 27%. Figure 4 shows the required specifics used in cell design [14], which we will be closely following. The HOP layer shows the same characteristics of an n-type with doping concentration, N_D = 10^{13} $cm^{-3,}$ and diffusion length of 700 nm.

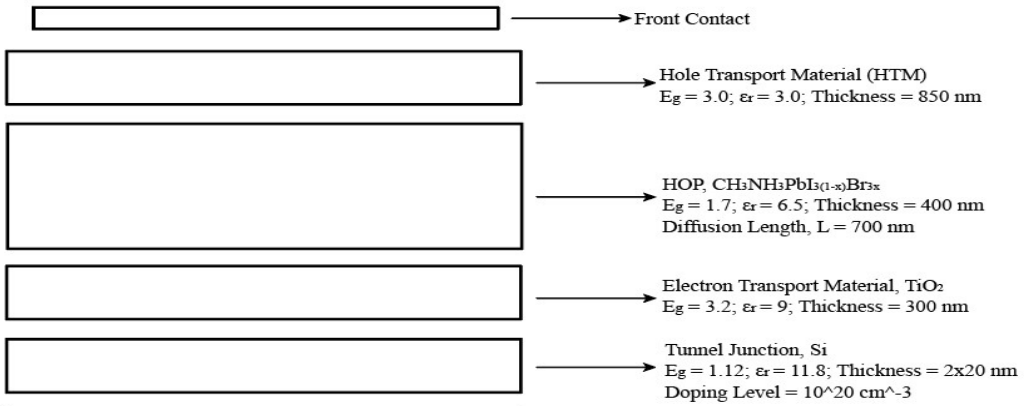

Fig.4: Cell Structure for PV Module.

For the implementation of this tandem cell in a PV module, we chose a simple 36 (9x3) design connected in series; a 3.2mm tempered glass panel with low iron oxide with an anti-reflective coating as the front surface material due to the low reflectivity, high transmissivity, strength, durability and self-cleaning properties [19]; Polyvinyl fluoride (commonly referred to as 'Tedler') as the back surface of the module as it is operational in an extensive temperature range (-70 °C – 110 °C) and has the following properties: high weather resistance, transparency, inherent strength and low permeability of moisture, vapor, and oil [18]; 2 sheets of Ethyl vinyl acetate ($(C_2H_4)_n(C_4H_6O_2)_m$) as the adhesive between the front and back surface which has optical transparency and low thermal resistance, and finally aluminum as the frame that protects the module from lightning storms (since Al has good conductive properties) and corrosion [19]. Figure 5 (a) and (b) show the structure of our proposed module.

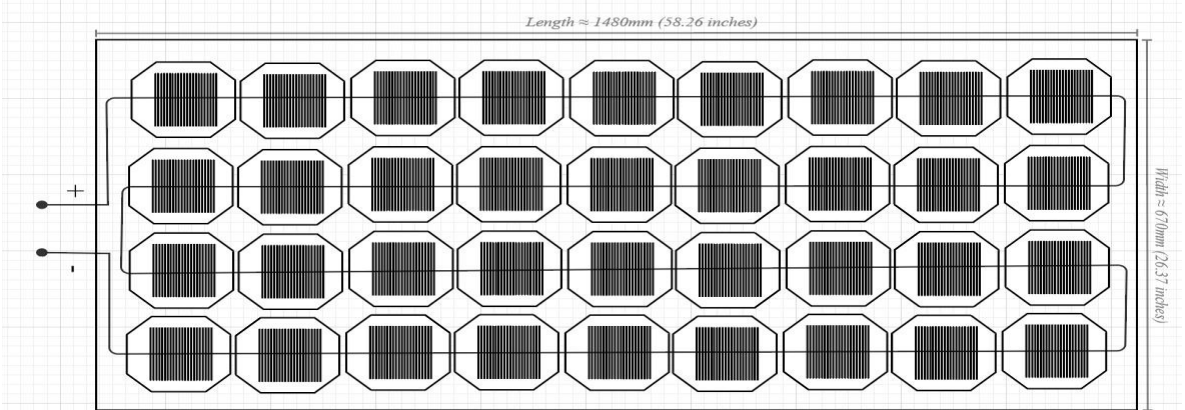

(a)

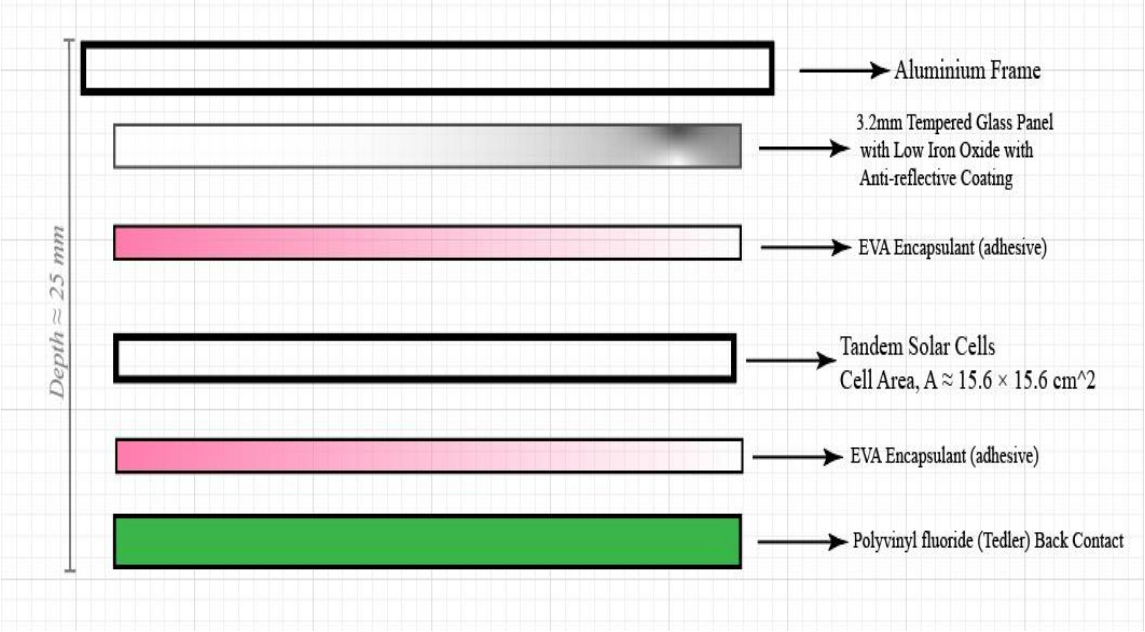

(b)

Fig.5: (a), (b) Top and Side View of the Proposed PV Module.

The total current $I_T = M.I_L - [e^{\frac{q\frac{V_T}{N}}{nkT}} - 1]$, where N is the number of cells in series; M is the number of cells in parallel; I_L = short circuit current from a single solar cell; I_0 = saturation current from a single solar cell; ideality factor, n= 1. From the equation, it is pretty evident that circuit current is largely dependent on the parallel connection. The total voltage equation can be easily derived and, consequently, the total power equation. All parameters relating to the tandem and cell and PV module under AM1.5 illumination are shown in Table 1**;** some of the values have been adapted from [14], the theories and relations applied to derive diffusivity, reflectivity, I_{sc}, P_{max} has been demonstrated in [19,20]. A PV cell also generates

heat as a result of being exposed to sunlight; the factors that contribute to heat generation are the reflection from the top surface of the module; the electrical operating point of the module; absorption of sunlight by the PV module in regions which are not covered by solar cells; absorption of low energy (infrared) light in the module or solar cells; and the packing density of the solar cells [19]. The temperature has a substantial impact on solar cells and panels; overheating reduces their efficiency dramatically [21]. Typically, 0.5% degradation of efficiency due to a 1°C surface temperature increase [22]. Figure 6, adapted from [23] shows, the effect of temperature on maximum cell power and voltage output.

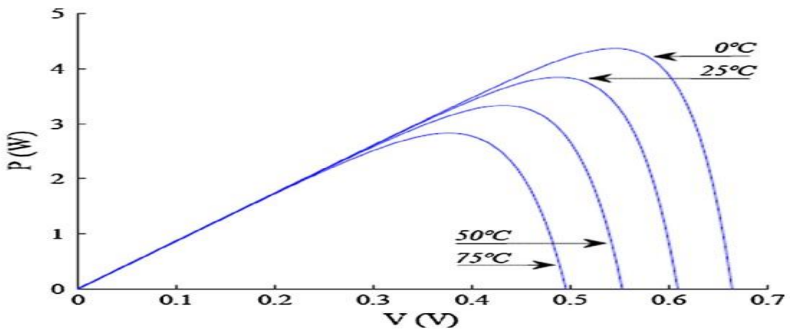

Fig.6: Degradation of Output as a Function of Temperature.

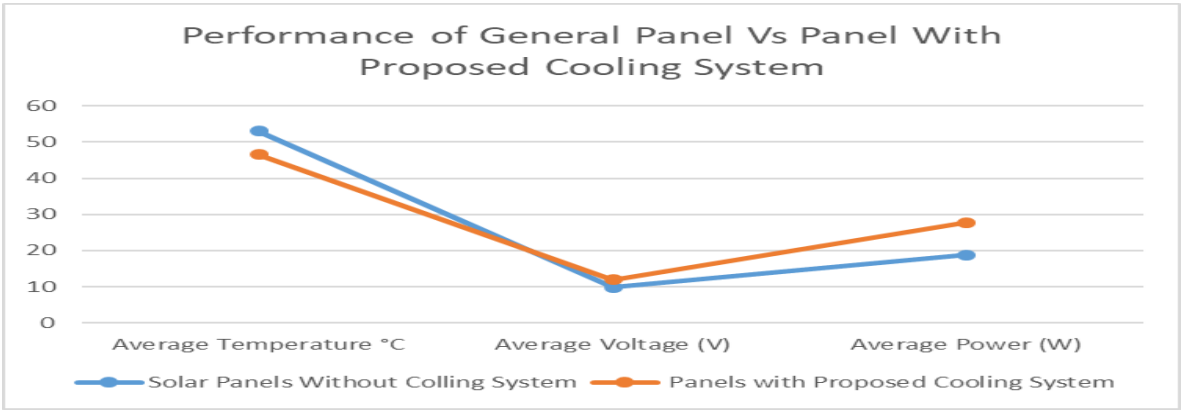

Fig.7: Temperature of a PV Cell is Largely Dependent on the Thermal Coefficient.

The effects of temperature on different cell parameters can be thoroughly understood by following [24], from where we can see that the temperature of a PV cell is largely dependent

on the thermal coefficient. A cooling system comprising of water in aluminum beams and a heat sink can be implemented to our PV module to get better performance from it. A straight fin heat-sink based model proposed in [26] can be used for reference. The results adapted from that experimental research are shown above in figure 7.

Because of geographical location, the sun's relative motion with respect to earth, atmospheric effects, getting constant solar irradiance is not possible [26], as an outcome radiant power density defined by $H = \int_0^\infty F(\lambda)d\lambda$ where F is the spectral irradiance. Therefore, using a sun tracker system (STS) to make the PV panel face the sun at all times for bolstering the maximum efficiency of our arrangement is necessary. STSs are more advantageous than traditional stationary LDR trackers, having almost 25% more performance ratings because LDR trackers are hindered by dust, shading by clouds, bird excrements, and reflected light of glass frames (e.g., windows) of buildings [27]. The GPS STS system proposed by P. I. Udenze et al. seemed a feasible option to us. The system is composed of a GPS module, a real-time clock (RTC) for reading date and time, a 5V dc 300ohm Stepper motor for solar module movement of 360°, an accelerometer (ADXL355) sensor as a positional feedback sensor of the motor, and a microcontroller for overall controlling of the system according to the Astronomical Equations of NREL Solar Position Algorithm. Table 3 in the results section shows the results of these equations for Dhaka, and Table 2 shows optimal tilt angles for maximum solar irradiance and mitigating cosign error.

Result and Discussion:

Table 1. Parameters relating to the tandem and cell and PV module under AM1.5 illumination.

Parameter	Value
E_g (eV)	1.7
Dark Current, J_o (A)	4.9×10^{-7}
$P_{sensitivity}$ (λ = 1200 – 8500nm)	~ .16
J_{sc} (Acm^{-2})	24.8×10^{-3}
Cell, I_{sc} (A)	6.03
Cell Area, A_{cell} (cm^2)	15.6 × 15.6
Cell, V_{oc} (V)	1.73
Fill Factor, FF_{cell}	0.849
Efficiency ($\eta\%_{cell}$)	26.6
$P_{max(cell)}$ (W)	8.8
Module/Panel Dimensions (HxWxD) (mm)	1480x670x25
$I_{sc(module)}$	~ 6
$V_{oc(module)}$	62.28
$P_{max(module)}$ (W)	~ 317.63

Table 2. Optimal tilt angles for maximum solar irradiance and mitigating cosign error.

Division	**One Tilt Angle for the Whole Year System**	**Two Tilt Angles for Two Halves of a Year System**		
	Optimum Tilt Angle (January December)	**Optimum Tilt Angle (April September)**		**Optimum Tilt Angle (October March)**
Dhaka	21.40°	8.70o		37.90°
Chittagong	20.20°	7.20°		36.40°

Rajshahi	22.10°	9.30°	38.50°
Khulna	20.70°	7.80°	37.00°
Barisal	20.60°	7.70°	36.90°
Sylhet	22.50°	9.80°	39.00°
Mymensingh	22.40°	9.70°	38.90º
Rangpur	23.30°	10.70°	39.80º

Table 3. Result based on Astronomical Equations of NREL Solar Position Algorithm.

Hour	**Elevation**	**Azimuth**
5:23:31	-0.833	100.51
6:00:00	5.96	106.45
7:00:00	16.64	116.97
8:00:00	26.27	129.11
9:00:00	34.21	143.64
10:00:00	39.57	160.97
11:00:00	41.43	180.36
12:00:00	39.4	199.7
13:00:00	33.9	216.91
14:00:00	25.87	231.32
15:00:00	16.17	243.35
16:00:00	5.45	253.8
16:33:40	-0.833	259.26

Although 2.2 W/m^2 was shown to be feasible, the exact parameters were not specified. Many factors still need to be reevaluated before effectively implementing the model in different systems. The TEG achieves a temperature difference of 7.5 K (300-293.1) at 300 K and 7.0 K at 292.5 K and a power density, P_{max} of 1.2144 W/m^2. During the daytime, by using the three-layered upper side, an efficiency of 15.7% can be achievable, which is significantly high considering the device's potential to generate a high amount of power at 100 suns due to the immense value of ΔT, this performance can be further bolstered by using materials produced by novel technologies. A predicted efficiency of 23.5% for a material with ZT=2 has been stated in [11]. For the PV module, the effect on different parameters due to sun tracking and cooling system needs to have further experimented, and we believe a much larger power density than the calculated 0.32 $mAmm^{-2}$ of a standalone panel (without cooler or tracker) can be obtained by measurement and simulation. Inverters, storage systems (batteries), and boost converters for total arrangement, and a total simulation of the system

for finding all required figures and parameters will be done in due course. The materials and pattern for the Solar Thermoelectric Photovoltaic Tree (STPT) have to be selected after deep consideration. However, for the preliminary stages, steel as the material and phyllotaxy patterns could be used. Figure 8 shows the transformation of TEG from its night to daytime working configuration, and a simple schematic of the proposed STPT is shown in figure_9 (a), (b), and (c).

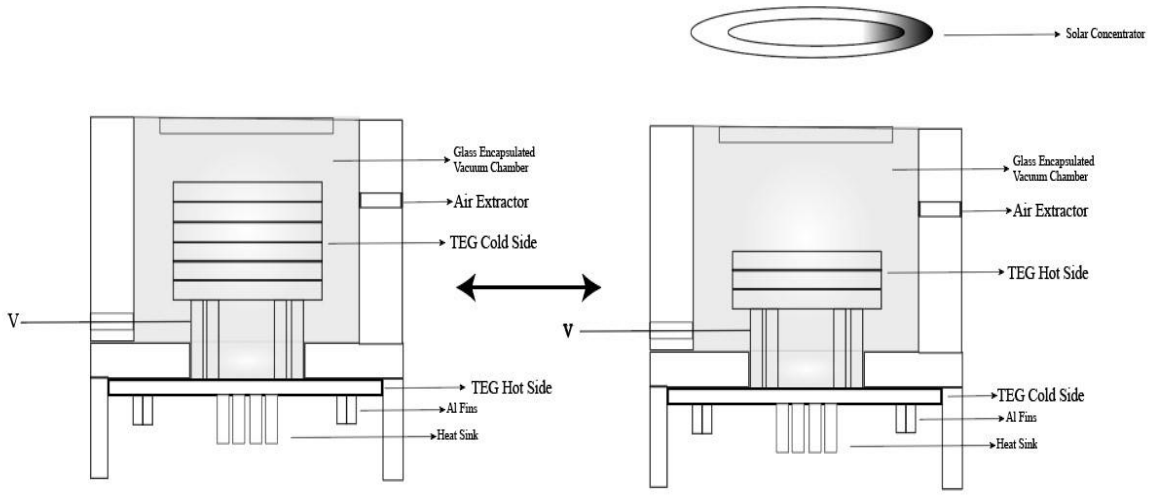

Fig.8: Device Transformation.

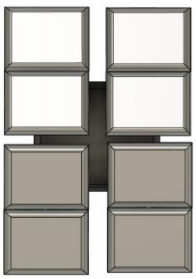

(a)

(b)

(c)

Fig.9: (a), (b), and (c) Top, Side, and 3D view of Solar Thermoelectric Photovoltaic Tree.

Conclusion: We get 173K Terawatts of power from the sun in just one hour, while the global energy consumption is 16T Watts, which means, if we could use the sun's total hourly power, we would not need to generate any excess power for about one year. In this paper, we have discussed one of the many directions of harvesting the sun's energy efficiently to answer our energy needs. This paper is more of a hypothetical work than extensive research, and by giving adequate time and opportunities, we are optimistic that we could validate all specifics of our model and realize its physical terms in the future. Our target is to influence our peers into exploring this field meticulously for fulfilling our energy needs on both national and international levels by their research as much work is still in process or left relating to the combination of energy harvesting at all times of a day.

Acknowledgments: We would like to show gratitude to our friend Mehedi Hasan for his assistance.

References:

[1]. IPCC (2014). Climate Change 2014: Mitigation of Climate Change. DOI: https://doi.org/10.1017/CBO9781107415416

[2]. OECD (Organisation for Economic Co-operation and Development). 2012. CLIMATE CHANGE. OECD Environmental Outlook to 2050 (pp. 5). DOI: https://doi.org/10.1787/9789264122246-en

[3]. USGCRP 2014, Third Climate Assessment.

[4]. USGCRP 2017, Fourth Climate Assessment.

[5]. Hoegh-Guldberg, Ove ; Jacob, Daniela ; Taylor, Michael ; Bindi, Marco ; Brown, Sally ; Camilloni, Ines ; Diedhiou, Arona ; Djalante, Riyanti ; Ebi, Kristie L. ; Engelbrecht, Francois ; Guiot, Joel ; Hijioka, Yasuaki ; Mehrotra, Shagun ; Payne, Antony ; Seneviratne, Sonia I. ; Thomas, Adelle ; Warren, Rachel F. ; Zhou, Guangsheng ; Tschakert, Petra. / Impacts of 1.5ºC global warming on natural and human systems. Global Warming of 1.5°C: An IPCC Special Report on the impacts of global warming of 1.5°C above pre-industrial levels and related global greenhouse gas emission pathways, in the context of strengthening the global response to the threat of climate change, sustainable development, and efforts to eradicate poverty . IPCC, 2018.

[6]. Stern, N. (2006). The Economics of Climate Change: The Stern Review, HM Treasury, Cambridge University Press, Cambridge, UK.

[7]. OECD. 2012. CLIMATE CHANGE. OECD Environmental Outlook to 2050 (pp. 15). DOI: https://doi.org/10.1787/9789264122246-en

[8]. D Enescu. (2019). Thermoelectric Energy Harvesting: Basic Principles and Applications. IntechOpen. DOI: http://dx.doi.org/10.5772/intechopen.83495

[9]. A. P. Raman, W. Li, and S. Fan, “Generating light from darkness,” Joule 3, 2679 – 2686 (2019). DOI: https://doi.org/10.1016/j.joule.2019.08.009

[10]. Orr B, Akbarzadeh A, Mochizuki M, Singh R. A review of car waste heat recovery systems utilizing thermoelectric generators and heat pipes. Applied Thermal Engineering. 2016;101:490-495. DOI: 10.1016/j.applthermaleng.2015.10.081.

[11]. L L Baranowski, G J Snyderb, E S Toberer. Concentrated solar thermoelectric generators. Energy Environ. Sci., 2012, 5, 9055. DOI: 10.1039/c2ee22248e.

[12]. Cheng TC, Cheng CH, Huang ZZ, Liao GC. Development of an energy saving module via combination of solar cells and thermoelectric coolers for green building applications. Energy. 2011;36(1):133-140. DOI: 10.1016/j.energy.2010.10.061.

[13]. L Fan, W Li, W Jin, M Orenstein, S Fan (2020). Maximal nighttime electrical power generation via optimal radiative cooling. Optics Express. (17, pp. 25460-25470). DOI: 10.1364/OE.397714.

[14]. A. Rolland, L. Pedesseaul, A. Beck, M. Kepenekian, C. Katan, Y Huang, S. Wang1, C. Cornet1, O. Durand, and J. Even (2017). Computational design of high performance hybrid perovskite on silicon tandem solar cells. DOI: 10.1109/NUSOD.2017.8009994.

[15]. S. Chen, L. Zhu, M. Yoshita, T. Mochizuki, C. Kim, H. Akiyama, et al., Thorough subcells diagnosis in a multi-junction solar cell via absolute electroluminescence-efficiency measurements, Sci. Rep. 5 (2015). DOI:10.1038/srep07836.

[16]. L.C. Hirst, N.J. Ekins-Daukes, Fundamental losses in solar cells, Prog. Photovolt. Res. Appl. 19 (2011) 286–293. doi:10.1002/pip.1024.

[17]. F. Dimroth, M. Grave, P. Beutel, U. Fiedeler, C. Karcher, T.N.D. Tibbits, et al., Wafer bonded fourjunction GaInP/GaAs//GaInAsP/GaInAs concentrator solar cells with 44.7% efficiency, Prog. Photovolt. Res. Appl. 22 (2014) 277–282. doi:10.1002/pip.2475.

[18]. N D Weimer (n.d.). TPT - Tedlar Polyester Tedlar: what is it? https://sinovoltaics.com/learning-center/materials/tpt-tedlar-polyester-tedlar-what-is-it/

[19]. C.B.Honsberg and S.G.Bowden, "Photovoltaics Education Website," www.pveducation.org, 2019.

[20]. S A Kalogirou (2014). Photovoltaic Systems. Solar Energy Engineering (Second Edition) Processes and Systems (pp. 481-540). DOI: https://doi.org/10.1016/B978-0-12-397270-5.00009-1

[21]. Akbarzadeh A, Wadowski T. Heat-pipe-based cooling systems for photovoltaic cells under concentrated solar radiation. Appl Therm Eng 1996;16(1):81–7. DOI: 10.1016/1359-4311(95)00012-3.

[22]. A. Pradhan, S. K. S. Parashar, S. M. Ali and P. Paikray, "Water cooling method to improve efficiency of photovoltaic module," 2016 International Conference on Signal Processing, Communication, Power and Embedded System (SCOPES), Paralakhemundi, India, 2016, pp. 1044-1047, doi: 10.1109/SCOPES.2016.7955600.

[23]. Rodrigues EMG, Melı´cio R, Mendes VMF, Catala˜ o JPS (2011). Simulation of a solar cell considering single-diode equivalent circuit model. In: International conference on renewable energies and power quality, Spain, 13–15.

[24]. D L King, J A, Kratochvil, W E Boyson (1997). TEMPERATURE COEFFICIENTS FOR PV MODULES AND ARRAYS: MEASUREMENT METHODS, DIFFICULTIES, AND RESULTS. Sandia National Laboratories.

[25]. S A Rakino, S Suherman, S Hasan, A H Rambe, Gunawan (2017). A passive cooling system for increasing efficiency of solar panel output. DOI:10.1088/1742-6596/1373/1/012017.

[26]. A. Sharma, 'Design of an Automatic Solar tracking controller Solar tracking controller', pp. 505–510, 2017.

[27]. Abid, A.J. (2017). Arduino Based Blind Solar Tracking Controller. International Journal of Open Information Technologies, 5, 24-29.

[28]. N. P. Sergeant, O. Pincon, M. Agrawal and P. Peumans, Design of wide-angle solar-selective absorbers using aperiodic metal-dielectric stacks, Opt. Express, 2009, 17, 22800–22812.

[29]. H. Sai, H. Yugami, Y. Kanamori and K. Hane, Solar selective absorbers based on two-dimensional W surface gratings with submicron periods for high-temperature photothermal conversion, Sol. Energy Mater. Sol. Cells, 2003, 79, 35–49 https://www.cei.washington.edu/education/science-of-solar/perovskite-solar-cell/